

A data-driven probabilistic model for well integrity management
case study and model calibration for the Danish sector of North Sea

Miraglia, Simona

Published in:
Journal of Structural Integrity and Maintenance

DOI (link to publication from Publisher):
[10.1080/24705314.2020.1746013](https://doi.org/10.1080/24705314.2020.1746013)

Creative Commons License
CC BY-NC-ND 4.0

Publication date:
2020

Document Version
Accepted author manuscript, peer reviewed version

[Link to publication from Aalborg University](#)

Citation for published version (APA):
Miraglia, S. (2020). A data-driven probabilistic model for well integrity management: case study and model calibration for the Danish sector of North Sea. *Journal of Structural Integrity and Maintenance*, 5(2), 142-153. <https://doi.org/10.1080/24705314.2020.1746013>

General rights

Copyright and moral rights for the publications made accessible in the public portal are retained by the authors and/or other copyright owners and it is a condition of accessing publications that users recognise and abide by the legal requirements associated with these rights.

- Users may download and print one copy of any publication from the public portal for the purpose of private study or research.
- You may not further distribute the material or use it for any profit-making activity or commercial gain
- You may freely distribute the URL identifying the publication in the public portal -

Take down policy

If you believe that this document breaches copyright please contact us at vbn@aub.aau.dk providing details, and we will remove access to the work immediately and investigate your claim.

A data driven probabilistic model for well integrity management: case study and model calibration for the Danish sector of North Sea

The correct functioning of well completion in oil and gas facilities, is eminently important to assure continuity of production operations together with an adequate safety level.

To enhance the performance of production wells and reduce maintenance expenditures, a shift of paradigm from corrective maintenance to a proactive risk based maintenance is necessary. In order to investigate the feasibility of fully probabilistic risk based inspection planning approach for subsea wells, a pilot study has been carried out at Danish Hydrocarbon Research and Technology Centre (DHRTC). After establishing a baseline for the system taxonomy, failure modes and their dependencies on deterioration mechanisms, a data collection and analysis lead to the calibration of a corrosion probabilistic model, based on pit-size measured from tubing inspections. This manuscript presents the results of the feasibility study, the calibration of a bespoke corrosion model for wells in the Danish sector of North Sea, the reliability analysis (pressure burst failure) and the identification of a threshold value for the pit penetration to be compared with current O&G regulations. The model is further used to compare expected maintenance costs for two policies, namely corrective maintenance, which is the most used policy in O&G companies, and condition based maintenance. Results show how the condition based maintenance policy results in lower maintenance costs and potential extension of well lifetime.

Keywords: ageing of oil&gas production tubing; corrosion; corrective vs condition based maintenance policy; life cycle costs

Introduction

Risk based inspection planning (RBI) has been widely used for the integrity management of transportation infrastructures and pipelines networks, offshore structures such as platforms and wind turbines. However, in the context of sub-sea and/or sub-surface well integrity, this method is seldom applied and risk assessment is used mostly in a qualitative and semi-quantitative way when aiming at programming workovers (Pedersen et al.,

2012, Chilingar, 2013). This testifies the need for a shift of paradigm from reactive/corrective maintenance of the sub-surface wells to a proactive risk based maintenance to ensure and enhance performance. Indeed, the use of probabilistic methods and risk based management approach facilitates this paradigm shift by allowing formulating the best strategy aiming at obtaining the desired performance for the asset with respect to a defined service level and safety acceptance criteria (Straub, 2007). The best maintenance strategy in RBI is obtained as the optimal strategy according to a classical decision analysis optimization problem, where the objective is to minimize the risk function, and where risk is defined as the expected value of the consequences associated to a specific failure mode and therefore is proportional to the probability of the failure mode and costs.

In order to investigate the feasibility of the use of risk based maintenance for the North Sea production wells, an extensive data collection has been performed aiming at gaining both qualitative information in the form of expert opinions and quantitative data from inspections with logging tools performed during workover operations. The data collected permitted the calibration of a bespoke probabilistic corrosion failure model targeting the simulation of pit maxima whose presence might cause the bursting of the tubing with consequent leak, loss of integrity and trigger therefore a workover.

This manuscript consists of two parts. First the data collected is analysed and the corrosion model is developed. In the second part the model is used to simulate the probability of failure for burst over the fixed 30yrs life span, with corresponding costs of maintenance for two policies: corrective maintenance and condition based maintenance (with perfect information).

54 *Phenomenology of corrosion process*

55 Multiple studies are available in literature where the need for modelling the corrosion
56 process as time and spatial variant problem is addressed. In particular, the dependency of
57 the corrosion rate on multiple variables governing the corrosion phenomena is widely
58 acknowledged. However, in both field and laboratory observations, often the recording
59 of data is not done in a consistent way, making difficult the derivation of models able to
60 comprise those dependencies. Temperature and flow velocity are identified as most
61 important parameters governing initiation of corrosion in both sea water exposed
62 elements and in transportation pipelines and tubing (Melchers, 2003a, Chilingar et al,
63 2013). The uncertainties related to these variables propagates to the corrosion process,
64 where both spatial variability and time dependency can be observed. In particular,
65 corrosion losses vary almost linearly in time, with standard deviation of corrosion losses
66 showing a linear increase with the exposure time.

67 Different models for the growth rate of uniform and pit corrosion are available, especially
68 for the offshore industry (Olsen, 2003, Melchers, 2003a,b, Smith, 2005, Nešić, 2007,
69 Nyborg, 2010). In this context, Engelhart&MacDonald(2004), have widely highlighted
70 the need for the combination of mechanistic and statistical models pointing at advantages
71 and disadvantages of both approaches. Mechanistic and empirical models have the
72 advantage of being built on the interpretation of the corrosion phenomena and address
73 clearly the dependencies among the variables. Statistical models, are often not based on
74 phenomenological models, but can capture the correlation among variables and track
75 evolution over time of the phenomena. However, while in mechanistic models, model
76 parameters represent physical variables of the problem (e.g. corrosion pit depth),
77 parameters of statistical models (e.g. EV distributions) do not represent physical
78 variables, but statistic characterization of the dataset used (Engelhart&MacDonald,

2004). Therefore, statistic models may have limited validity depending on the extension of the dataset and may not be able to capture the full evolution over time of the phenomena, due to both limitation of the dataset and of extrapolation method itself. Especially, since statistic distribution parameters do not have physical meaning, no direct observation can be done and consequently, the use of Bayesian updating to improve the model is not straightforward (Melchers, 2003a, Engelhart, 2004). Therefore, the mechanistic model should be combined with statistical calibration on in-situ data.

A power function of the time $a \cdot t^\beta$ is commonly used to model the evolution of corrosion pit depth (see Laycock, 1990, Melchers, 2003a, 2003b, 2004, Engelhardt, 2004, Straub, 2007), with factor β calibrated by regression on experimental data and considered deterministic. Indeed, both Laycock (1990) and Melchers (2008) highlight that β should be kept constant (0.5) for pure hypothesis of Fickian diffusion homogenous process. Moreover, Melchers (2003a) underlines the importance of using in-situ data because the organic compound is too difficult to reproduce in lab test and short term lab-test will lead to misinterpretation of long term corrosion process.

Figure 1 illustrates the phenomenological evolution of corrosion losses (see Melchers 2003a, 2003b). The initial phases 0 and 1 account for initial effects of oxygen on the surface (kinetic phase) in which micro-pitting appears very rapidly; phase 2 is then leaded by the rate of oxygen penetration into the corroded surface, phases 3 and 4 are rapid and steady state progression of pit growth. In particular, experimental data from Melchers (1999 to 2008) demonstrated how bacteria associated with corrosion have optimal metabolism at temperatures between 25 and 30°C, while the activity is very low at 5°C and above 50°C, with no corrosion at freezing temperatures (-2°C). However, these temperature values are much lower than operating temperature of oil production tubing,

where bacterial concentration is also very low due to the use of nitrogen and bactericide.

When seeking to optimize an inspection and maintenance strategy, corrosion losses and the rate of corrosion during the intermediate phases (from initial kinetic phase to end of life) are key variable and estimating corrosion losses based only on corrosion rate may lead to big erroneous evaluations (Straub, 2007, Melchers, 2008). It can be argued that (Figure 1), using the rate calculated on short-term lab test data (initial corrosion phase), will likely lead to overestimating the corrosion rate, therefore leading to the planning of inspections and maintenance operation at small time intervals, which will not be realistic. On the contrary, considering only a secant value of corrosion rate (i.e. roughly calculated as ratio between end-of-life corrosion loss and age of the tubing), leads to a good estimate of an average corrosion rate, but not of higher rates during steady state corrosion propagation, where one may want to act using inhibitors in order to control the corrosion rate.

Choice of probabilistic distribution in corrosion modelling

The choice of the probabilistic distribution used to model time to failure and degradation process has large influence on the resulting reliability (Quesenberry, 1982, Rausand, 1998). The use of Lévy process (especially Gamma) to simulate deterioration of components has been largely suggested (Williams et al, 1985, Pandey et al, 2005, Noortwijk et al., 2007, Amaya-Gómez et al., 2019, Oumouni et al, 2019). Main advantage of using Gamma distribution lays in the easier inclusion of time variation through the shape parameter, while keeping constant the scale parameter. However, a Gamma process has independent positive increments, which makes realizations monotonic and linearly increasing, thus a dataset of progressive increments of defect size is needed to model the degradation process where any non-linearity of corrosion processes, , any variation of the

degradation rate and any dependency over operational parameters can be introduced by Bayesian updating whenever new observations are available (Pandey et al, 2005, Straub et al., 2007, Oumouni et al, 2019). The dataset available for this study does not provides increments of defect size in between inspections, but only pit sizes at failure, leading to the choice of a shock load type of distribution, as highlighted in the following sections.

Experimental evidence (Melchers, 2003-2008), showed how in the early phase of generation, pit location is Poisson-distributed with Exponential size, while full developed pits can have size following Normal, Lognormal and even Extreme Value distribution type. In particular, the data analysis done in Melchers (2005a) evidenced a bimodal behaviour of the pit size distribution, with an initial exponential distribution (first mode) combined with one or more normal components (for deeper pits). This behaviour is observed when data are clustered in homogenous populations, while mixed and inhomogeneous data (stable and metastable pits) would show better fit with extreme value distributions (especially Gumbel) due to the larger uncertainty associated with the observations (Scarf, 1996, Engelhardt, 2004, Melchers, 2005a).

A large debate therefore has been developing (Wang et al, 2003, Melchers, 2005a, Valor et al., 2007) on whether the Gumbel, Weibull or Frechet distributions can be used as realistically representative for the pit depth distribution. The objection to the use of EV distribution, or single mode distributions in general, lays in the bad fit of the lower tail, causing the overestimation of the pit depth in the initial phase and reliability underestimation. Despite being an open discussion, a solid conclusion is that on the basis of data regression and classic statistical test, Weibull and Frechet distribution do not adequately represent the distribution of pit depths while Gumbel distribution or Gaussian mixture can be used with a good fit. On the contrary, regarding spatial distribution and generation rate over time, opposite findings can be found (Williams 1985, Valor et al.,

2007,Taratseva, 2010) as a consequence of the difficulties modelling the incubation period of the pits, when pits generates fast and at non-homogenous rate. Table 1 summarizes the most relevant used probability distributions in corrosion modelling.

Melchers (2003a), proposed a complex model for corrosion losses based on a time dependent three components stochastic function containing a deterministic mean function, a Boolean bias function and a zero-mean uncertainty function depending on environmental parameters such as temperature, steel composition, surface finishing etc. However, a large dataset comprising all environmental parameters would be necessary to calibrate the model. Such dataset could be available for large experimental campaigns, but rarely as field data. Moreover, the dependency of corrosion rate on time and environmental conditions should be carefully investigated by means of e.g. multivariate analysis, principal component analysis, multiple predictor and bundling methods (Liu et al., 2009, Jiménez-Come et al., 2012) to avoid redundant information and that the error function is biased by not differentiating the contributions from model error and approximation, measurement errors, spatial variability and statistical uncertainty, thus leading to the limitations highlighted in Engelhart (2004).

The DHRTC research activity on North Sea oil production wells

The Danish Hydrocarbon Research and Technology Centre (DHRTC) supported an extensive data collection. The baseline for system boundaries identification, components taxonomy and failure modes and deterioration mechanisms for the well completion, d was established by a structured expert workshop.

Measurements collected during the preparation for workover phase and during inspection campaign have been made available by DHRTC/Mærsk/Total consortium. Data cover

two fields of the Danish sector of North Sea being operated with (Field 1) and without (Field 2) gas lifting of the production fluids.

A first set of measurements consists of size of maximum pit penetration with corresponding depth-location in the production tubing of oil producers (OP) with respective completion and inspection dates, obtained using multi-finger-calliper logging tool (MFC). The MFC consists of a tungsten body on which an array of flexible moving fingers are mounted to measure inner diameter of tubing and casing strings while logging it inside the well. Due to the lack of information over the calibration of the MFC, the measurement uncertainty is here not considered (i.e. perfect information).

A second set consists of measurements of daily maxima of operating pressure recorded by top head and bottom head pressure gauges.

The scope of using in-situ data is twofold: 1- learning the distribution of pit sizes at failure and operating pressure profile from observations; 2- calibrating the parameters of the Poisson occurrence of maxima pit sizes.

Analysis of survey data and probabilistic model calibration

As measurements of pit depth were obtained from different inspections made with potentially different MFC tools, it must be assumed that the measured pits represent independent observations of the same distribution of pit size, i.e. pit measured are all identically distributed (Laycock et al, 1990, Isogai, 2004, Melchers 2005a, Zhang, 2014, Ossai et al., 2016). Indeed, there is enough evidence that extreme pitting events at different hotspots occur as independent events (Turnbull, 1993, Melchers, 2003-2008, Jarrah et al, 2011), where any apparent correlation among extreme pits shall be interpreted as caused by uniform exposure rather than a real dependency (Melchers, 2005a). This hypothesis applies well to our dataset, since pits were measured during inspection for

workover preparations, meaning that, with few exceptions, tubings were all substituted after the inspections, and that measurements done in the same well at different times, do not correspond to the same pit.

The average maximum pit depth over time and along tubing depth is depicted in Figure 2 and Figure 3. Field 1 shows higher average of maxima pit size over a shorter life time respect to Field 2. The average pit size increases with exposure time for both fields in the short period, then decreases as a larger number of smaller pits are detected, then increases again due to detection of maxima pits. A hidden effect is the shrinking of population size for the 4.5in which have been progressively substituted by 5.5in. The increase is faster for the oil producers of 5.5in with respect to the 4.5in.

Correlation among exposure time (age), location depth size of pits was also investigated. Correlation of the pit size with depth is lower (10% to 30%), while a higher correlation (20% to 50%) is found with tubing age.

The pit maxima occurrence

Figure 2 and Figure 3 show pits are detected even after short exposure time. The high uncertainty in modelling nucleation rate over time makes it difficult to model initiation time from detected defects (Valor et al., 2007, Tarantseva, 2010).. Herein, the assumption of Normal distribution for the initiation time is made and the parameters in Table 2 were derived considering average time to occurrence of pits within the first five years of tubing exposure.

Under the hypothesis of independent observations, the number of pits $N(t)$ generated per well per year can be modelled as a Poisson point process (Benjamin&Cornell, 1970) with probability distribution in Eq.1, with mean rate of event λ in the interval $(0, t)$.

$$P(N(t) = n) = e^{-\lambda t} \frac{(\lambda t)^n}{n!}, n \geq 0 \quad (1)$$

The choice of a Poisson process lays in the fact that the available data consist of independent observations of maxima pit sizes at failure. This extreme type of defect is more correctly assimilated to shock loads in terms of occurrence (Poisson) rather than to a gradual degradation (increments) which instead should be modelled with Gamma process (Singpurwalla, 1997, Pandey et al., 2005). In addition, any peak over threshold approach, which would reduce uncertainty in the defect simulations with respect to the block maxima approach, (van Noortwijk et al, 2007), would converge to a Poisson process as the data consist of maxima over a selected threshold of pit size.

For both fields the occurrence of pits increases over time (see Figure 2 and Figure 3). Therefore, a linear function for the parameter λ is fit over time such that $\lambda(t) = a + bt$, with constants a and b listed in Table 3.

Maxima pit size distribution

Maximum likelihood algorithm (MLE) is used to estimate probability distribution parameters for the maximum pit size. The data (Figure 4 and Figure 5) show an evident bi-modal trend. Therefore, a two-component Gaussian mixture as in Eq.(2) is chosen. The calibrated parameters are listed in Table 4, where Φ_i represents the Normal distributed i -th component and π_i its weight.

$$F(d_p) = \sum_{i=1}^2 \pi_i \cdot \Phi_i(d_p) \quad (2)$$

To obtain faster convergence of the MLE, the standard deviation is constrained to be the same for all the components (see Table 4).

Due to the limited number of data points, any variation over time of the parameters of the distribution of pit sizes is omitted at this stage.

Maxima values of operating pressure

The probability distribution of operating pressure is calibrated on records from the gauges located at bottom head (BHP) and top head (THP) inside the wells. In Figure 6, the empirical marginal density functions of yearly maxima of the pressure at Top (THP) and Bottom (BHP) Head for Field 1 and Field 2 is depicted. As expected, BHP and THP show to be good correlated in both Fields. No significant variation over time of yearly maxima value is observed over 15 years of operation.

A Weibull marginal distribution is chosen (Eq.5) to model THP and BHP, on basis of best fit of data in the tails. The parameters are listed in Table 5 and Table 6, for Field 1 and Field 2 respectively.

In addition, two Normal distributed independent components ω_T and ω_B are added to simulate the fluctuation over time of the THP and BHP (Eqs.(3) & (4)). The two Normal components have zero mean and standard deviation equal to the sample standard deviation of THP and BHP (i.e. simple Gaussian increment, see Eqs.(6) & (7)).

$$THP(t) = w_{thp} + \omega_T(t) \quad (3)$$

$$BHP(t) = w_{bhp} + \omega_B(t) \quad (4)$$

$$w_{thp,bhp} = \frac{p_2}{p_1} \left(\frac{p}{p_1} \right)^{p_2-1} \exp \left(- \frac{p}{p_1} \right)^{p_2} \quad (5)$$

$$\omega_T = N(0, \sigma_{thp}^2) \quad (6)$$

$$\omega_B = N(0, \sigma_{bhp}^2) \quad (7)$$

Failure model, reliability analysis and evaluation of the maintenance strategy

The developed probabilistic model for corrosion is used for reliability analysis of one oil producer (tubing) with the aim of evaluating the best maintenance strategy between corrective maintenance (most used in O&G companies) and condition based maintenance (with perfect information). Main difference between corrective and condition based maintenance consists in the planning of workover operations (i.e. complete renewal of the tubing). In a corrective maintenance strategy, workovers are executed upon the

occurrence of the tubing failure, generally detected due to an anomaly in the wellhead functioning (e.g. pressure). In condition based maintenance, the workover is planned after an inspection where a detection is made of one or more corrosion pits exceeding a defined threshold.

The evaluation of the condition based strategy is made for two fixed inspection interval of 3 and 10 years and considering thresholds of pit size to thickness ratio of 60% and 80%. These values are chosen on the basis of requirements in Norsok Y-002 and DNV-GL/ST-F101, which indicate a minimum safety factor of 1.1 and 1.3 (high consequence class) respectively, with material partial safety factor of 1.15. On this basis, from the cumulative distribution of the pit size at burst (Figure 8-right), the corresponding thresholds of 80% and 60% are computed corresponding to the safety factors of 1.1 and 1.3.

Production tubing subject to internal corrosion, exhibit two main failure modes: leak due to pit growth to full thickness and burst due to reduced pressure capacity at the section contouring the defect (pit).

Several criteria are available to calculate the residual pressure capacity $p_c(t)$ at localized defects (Ahammed, 1996, Yong et al., 2001, Ossai et al., 2016). In absence of detailed information regarding the shape of the pits, the assumption of near rectangular pit with mean value of length l equal to $2d_p$ is made, while the effect of width of the defect can be neglected (Netto et al., 2005). In Eq.(8) and (9), σ_p and σ_f represent respectively the hoop stress at failure and the flow stress. The latter is a function of the material yielding stress as in Eq.(9) with the factor m_f ranging values 1.10÷1.15 (Ahammed, 1996). The concentration of stresses around a defect on the tubing surface is taken into account using the bulging or Folias factor M (Eq.(11), Yong et al., 2001).

$$\sigma_p(t) = \sigma_f \frac{1 - d_p(t)/t_n}{1 - d_p(t)/t_n M} \quad (8)$$

$$\sigma_f = m_f \sigma_y \quad (9)$$

$$p_c(t) = 2\sigma_p(t)t_n/D \quad (10)$$

$$M = \begin{cases} \sqrt{1 + 0.6275 \frac{l^2}{Dt_n} - 0.003375 \left(\frac{l^2}{Dt_n}\right)^2}, & \frac{l^2}{Dt_n} < 50 \\ 0.032 \left(\frac{l^2}{Dt_n}\right) + 3.3, & \frac{l^2}{Dt_n} > 50 \end{cases} \quad (11)$$

Two limit states functions describing leak and burst over time can be defined (Eq.(12) and Eq.(13) respectively). In Eq.(13), $p_c(t)$ indicates the residual capacity of the tubing with a defect and $p_s(t)$ indicates the service pressure at time t . The two mechanisms are considered to act in series.

$$g_l(\mathbf{X}, \mathbf{t}) = t_n - d_p(t) \quad (12)$$

$$g_b(\mathbf{X}, \mathbf{t}) = p_c(t) - p_s(t) \quad (13)$$

The tubing is modelled as a series system of sections containing a defect with changing dimensionality according to the number of sampled defects $N(t)$. A deterministic distance between top and bottom gauge is assumed ($L=7000\text{ftMDRT}$) and the location of maximum pit generated is considered uniformly distributed in the range 0-1000ftMDRT (approximation based on data observation).

The operating pressure $p_s(x_i, t)$ at location x_i of the pit i is considered linearly depending on the values THP and BHP as in Eq.(14).

$$p_s(x_i, t) = \left(\frac{x_i - L}{L}\right) [THP(t) - BHP(t)] \quad (14)$$

Figure 7 illustrates the simulation model and the simplified tubing geometry utilized. The variables of the probabilistic model are summarized in Table 7. The reliability analysis is performed with crude Monte Carlo for four cases:

- Field 1 with tubing 4.5inc;
- Field 1 with tubing 5.5inc;
- Field 2 with tubing 4.5inc;

- Field 2 with tubing 5.5inc.

Results of the numerical analysis and comparison of two maintenance strategies

The results of the numerical investigation comprise both reliability analysis and the evaluation of the two maintenance strategies. No occurrence of pure leaking failure is found, as it is rather the local bursting, due to the reduced resistance of the corroded tubing, to cause the creation of a hole and the leak of produced fluids.

In Figure 8, the cumulative probability distribution (CDF) of pressure (left) and pit size [in] at burst (right) are depicted. As expected, burst failure occurs with non negligible probability even for small pit size in the case of small tubing diameter ($D1=4.5\text{in}$) while the larger tubing ($D2=5.5\text{in}$) would generally fail for larger pits. A minimum threshold of 10% of wall thickness can already cause the failure in all considered cases. This is consistent with most O&G regulations imposing the evaluation of the safety level and corresponding maximum allowed operating pressure for corrosion defect of 10-80% of wall thickness (ASME-B31G,1991). In addition, D1 tubing in Field 1(gas lifted) shows high burst probability in the interval 10-30% pit depth to wall thickness ratio. Tubing D2 located in Field 2 (not gas lifted) shows high probability for lower values of depth to thickness ratio in combination with a higher reliability index, thus indicating that the failure of this tubing occurs only for high value of operating pressure (in the upper tail of pressure probability distribution). This is evident when looking at the cumulative probability distribution of the pressure values at burst event (Figure 8-left), showing that for D2 in Field 2, burst occurs with higher probability at higher values of pressure.

Figure 9, Figure 10 and Figure 11 depict the cumulative probability of failure over the 30yrs life time and the reliability index for the cases considered. As expected, failure probability is increasing over time with slower increase for Field 2. This is the effect of both a smaller number of detected pits in Field 2, symptom of slower corrosion rate, and

a higher uncertainty in the pit size and occurrence for Field 1. The failure probability and correspondent reliability index do not change significantly for the two maintenance strategies, neither for the two inspection intervals (3&10yr) for the condition based strategy (Figure 10, Figure 11). However, the gradient of failure probability is smaller for condition based policy, indicating that this strategy allows for a slower degradation of the tubing and smaller uncertainty. In particular, the smaller threshold for the defect size (60%) leads to a slightly higher reliability especially in the early stage of lifetime, where pits detected are more likely to be smaller than 80% of thickness and therefore the renewal of the system becomes more frequent.

The total costs per year for corrective and condition based maintenance strategies are evaluated. The influence of the discount rate and ratio between failure cost and workover cost is investigated. The evaluation of the discount rate in the appraisal of O&G investments is a complex task, which involves knowledge of the oil-field and company market value, company tax rate, market value of the interest-bearing debt of the company, etc. (Smith, 1999). Due to lack of detailed information, the values of 5%, currently most used rate in investment appraisal for O&G (Weijermars, 2013), and 11%, common risk adjusted rate in O&G(Smith, 1999) are used.

Workover costs might vary largely, depending on duration of operations and severity of damage. Indeed, there might be little difference between workover and failure costs, as the only possible repair is to substitute the full completion, and the cost of the rig per day is the major cost voice. Therefore, when cost of failure and cost of workover are comparable, a little difference in the life cycle costs among strategies is expected. When cost of failure largely differs from workover costs, a trade-off might be visible when comparing maintenance strategies. This is confirmed by the results of the simulations

(Figure 12 and Figure 14). In the following, for reason of conciseness, results are illustrated for Field 1 only, but same trend is found for Field 2.

The annual discounted cost of maintenance shows no difference among the strategies in the early lifetime with a bifurcation of the curve, which back-shifts when the discount rate increases and when failure costs are significantly larger than workover costs ($F=100WO$) (Figure 14, Figure 15). When failure costs and workover costs are comparable ($F=3WO$) (Figure 12, Figure 13) the cost per unit of time for the two maintenance strategies is almost the same with a slight gain choosing the condition based strategy with 10yrs inspection interval and 60% defect size to thickness ratio as acceptance threshold, as this allows for slightly higher reliability. The 80% threshold shows to be too high and results in terms of costs for this choice converge to the corrective maintenance (Figure 13).

For failure and workover cost of comparable magnitude, the annual cost of maintenance reaches a steady state value after 15yrs. For failure costs largely exceeding workover costs, the difference among the strategies becomes more evident with a cost curve resembling the classic failure bathtub curve (Figure 14, Figure 15).

Conclusions

The prediction of service life of tubing in offshore oil&gas production wells presents several challenges due to the specific operational condition and exposure to chemicals that vary from well to well, even in the same production field. Herein, results from the feasibility study for the application of condition based asset management is presented. Data has been collected for two fields: Field 1, characterized by gas lifted production and higher corrosion rate; Field 2, operated without gas lifting and with slower corrosion rate.

Results of the numerical analysis showed that gas lifted fields clearly exhibit higher probability of tubing failure due to the interaction of corrosion mechanisms weakening the tubing resistance with the pressure gradient caused by the gas-lifting procedure. For gas-lifted fields tubing with small diameter and thickness are not advised.

Expected costs per unit of time in corrective and condition based maintenance policies shows negligible difference in the early life (up to 10years). The cost reduction in condition based maintenance becomes more evident with the increase of life span of the asset, showing how it allows for both cost reduction and extension of the lifetime of the asset, whereas the value of the field is still of economic interest.

In particular, results demonstrated how for assets with repair (workover) costs much smaller than failure costs, the benefit from choosing a condition based maintenance policy is evident. In assets such as oil&gas wells, the workover costs are often comparable to the failure costs, making more difficult to evaluate the optimal maintenance strategy, which will likely be a combination of corrective and condition based policies.

It must be highlighted that the available data allowed only to estimate occurrence and size of pit maxima leading to a series of limitation in the results. First, an underestimation of the failure probability might be possible, because the effect of the resistance reduction of the tubing caused by smaller but more numerous pits (i.e. clusters and geometry effects) is neglected. This underestimation may be affecting mostly the assessment of Field 2, where the damage of smaller pits may cause more failures than evaluated with this model, while for Field 1, due to the higher operating pressure, this effect may be irrelevant as it could be hidden in the burst failure mode. Indeed, discarding pit geometry by using only pit penetration depth simplifies the problem by reducing its dimensionality, but does not allow to take into account for area losses neither to estimate the number of pits per unit area and the local effect of pit clusters. Therefore, the use of full available information

collected during inspections shall be used (all pit measurement of depth and full geometry). This in combination with adequate information on the uncertainty of measurement from the caliper, would certainly allow for the optimization of inspection intervals and of the best maintenance policy, bespoke for each production field. In addition, a sensitivity analysis on measurement uncertainty and on estimates of future production (economic value of the field) could be of interest for further analysis.

Acknowledgements

The author would like to express gratitude to the Danish Hydrocarbon Research and Technology Centre, and A.P.-Møller-Mærsk/ Total for providing the necessary data and financial support. Special thanks to Prof. J. D. Sørensen (Aalborg University) for his comments on the manuscript.

References

Ahammed, M., & Melchers, R. E., 1996, 'Reliability estimation of pressurised pipelines subject to localised corrosion defects'. International Journal of Pressure Vessels and Piping, 69(3), 267-272.

Amaya-Gómez, R., Riascos-Ochoa, J., Munoz, F., Bastidas-Arteaga, E., Schoefs, F., & Sánchez-Silva, M. (2019). Modeling of pipeline corrosion degradation mechanism with a Lévy Process based on ILI (In-Line) inspections. International Journal of Pressure Vessels and Piping, 172, 261-271.

ASME B31G (1991), "Manual for Determining the Remaining Strength of Corroded Pipelines", ASME B31G-1991, New York, 1991.

Benjamin, J. R., & Cornell, C. A., 1970, 'Probability, statistics, and decision for civil engineers'. McGraw Hill.

434 Caleyó, F., Velázquez, J. C., Valor, A., & Hallen, J. M., 2009. Probability distribution
 435 of pitting corrosion depth and rate in underground pipelines: A Monte Carlo study.
 436 Corrosion Science, 51(9), 1925-1934.

437 Chilingar, G. V., Mourhatch, R., & Al-Qahtani, G. D., 2013, 'The fundamentals of
 438 corrosion and scaling for petroleum and environmental engineers', Gulf Publishing
 439 Company, 2 Greenway Plaza, Suite 1020, Houston. TX 77046.

440 DNVGL-ST-F101., 2017. Submarine pipeline systems. Available at
 441 <https://www.dnvgl.com/rules-standards/>

442 Engelhardt G., MacDonald D.D., 2004, 'Unification of the deterministic and statistical
 443 approaches for predicting localized corrosion damage. I. Theoretical foundation',
 444 Corrosion science, 46(11),2755-2780.

445 Isogai, T., Katano, Y., & Miyata, K., 2004, Models and inference for corrosion pit
 446 depth data. Extremes, 7(3), 253-270.

447 Jarrah, A., Bigerelle, M., Guillemot, G., Najjar, D., Iost, A., & Nianga, J. M., 2011. A
 448 generic statistical methodology to predict the maximum pit depth of a localized corrosion
 449 process. Corrosion Science, 53(8), 2453-2467.

450 Jiménez-Come, M. J., Muñoz, E., García, R., Matres, V., Martín, M. L., Trujillo, F.,
 451 & Turias, I. (2012). Pitting corrosion behaviour of austenitic stainless steel using artificial
 452 intelligence techniques. Journal of Applied Logic, 10(4), 291-297.

453 Laycock, P. J., Cottis, R. A., & Scarf, P. A., 1990, Extrapolation of extreme pit depths
 454 in space and time, Journal of the Electrochemical Society, 137(1), 64-69.

455 Liu, Z., Sadiq, R., Rajani, B., & Najjaran, H. (2009). Exploring the relationship
 456 between soil properties and deterioration of metallic pipes using predictive data mining
 457 methods. Journal of Computing in Civil Engineering, 24(3), 289-301.

458 Melchers, R.E., 1999. Corrosion uncertainty modelling for steel structures. Journal of
459 Constructional Steel Research, 52(1), 3-19.

460 Melchers, R.E., 2003a. Modeling of marine immersion corrosion for mild and low-
461 alloy steels--part 1: Phenomenological model. Corrosion; Apr 2003; 59, 4.

462 Melchers, R.E., 2003b. Modeling of marine immersion corrosion for mild and low-
463 alloy steels--part 2: Uncertainly estimation. Corrosion; Apr 2003; 59, 4.

464 Melchers, R.E., 2003c. Probabilistic Models for Corrosion in Structural Reliability
465 Assessment—Part 1: Empirical Models. Journal of Offshore Mechanics and Arctic
466 Engineering, 125(4), 264-271.

467 Melchers, R.E., 2003d. Probabilistic models for corrosion in structural reliability
468 assessment—Part 2: models based on mechanics. Journal of offshore mechanics and
469 arctic engineering, 125(4), 272-280.

470 Melchers, R.E., 2005a, 'Statistical Characterization of Pitting Corrosion-Part 1: Data
471 Analysis', Corrosion; Jul 2005; 61, 7.

472 Melchers, R.E., 2005b, 'Statistical Characterization of Pitting Corrosion-Part 2:
473 Probabilistic modeling for maximum pit depth', Corrosion; Aug 2005; 61, 8.

474 Melchers R.E., 2008. Development of new applied models for steel corrosion in
475 marine applications including shipping, Ships and Offshore Structures, 3:2, 135-144,
476 DOI: 10.1080/17445300701799851

477 Nesic S., 2007, Key issues related to modelling of internal corrosion of oil and gas
478 pipelines – A review, Corrosion Science 49 (2007) 4308–4338.

479 Netto, T. A., Ferraz, U. S., & Estefen, S. F., 2005. The effect of corrosion defects on
480 the burst pressure of pipelines. Journal of constructional steel research, 61(8), 1185-1204.

481 Noortwijk (van), J. M., van der Weide, J. A., Kallen, M. J., & Pandey, M. D., 2007.
482 Gamma processes and peaks-over-threshold distributions for time-dependent reliability.
483 Reliability Engineering & System Safety, 92(12), 1651-1658.

484 NORSOK Standard, 2010. Y-002: Life Extension for Transportation Systems.

485 Nyborg R., 2010, CO₂ Corrosion models for oil and gas production systems,
486 Corrosion NACE International, Paper No-10371.

487 Olsen, S., 2003. CO₂ Corrosion Prediction by Use of the NORSOK M-506 Model-
488 Guidelines and Limitations. In CORROSION 2003. Nace International.

489 Oumouni, M., Schoefs, F., & Castanier, B. (2019). Modeling time and spatial
490 variability of degradation through gamma processes for structural reliability assessment.
491 Structural Safety, 76, 162-173.

492 Ossai, C. I., Boswell, B., & Davies, I. J., 2016. ‘Application of Markov modelling and
493 Monte Carlo simulation technique in failure probability estimation—A consideration of
494 corrosion defects of internally corroded pipelines’. Engineering Failure Analysis, 68,
495 159-171.

496 Pandey, M. D., Yuan, X., & Van Noortwijk, J. M., 2005. Gamma process model for
497 reliability analysis and replacement of aging structural components. Proceedings
498 ICOSSAR, Rome, Italy, Paper, (311).

499 Pedersen, H., 2012, Halfdan Corrosion Review. Maersk report: Rev.3.0-MOG-
500 AHA12-223.

501 Quesenberry, C. P., & Kent, J. (1982). Selecting among probability distributions used
502 in reliability. Technometrics, 24(1), 59-65.

503 Rausand, M., 1998. Reliability centered maintenance. Reliability Engineering &
504 System Safety, 60(2), 121-132.

505 Scarf P.A. & Laycock P.J., 1996. Estimation of extremes in corrosion engineering,
506 Journal of Applied Statistics, 23:6, 621-644, DOI: 10.1080/02664769623982.

507 Singpurwalla, N. (1997). Gamma processes and their generalizations: an overview. In
508 Engineering probabilistic design and maintenance for flood protection (pp. 67-75).
509 Springer, Boston, MA.

510 Smith, J. E., & McCardle, K. F., 1999. Options in the real world: Lessons learned in
511 evaluating oil and gas investments. Operations Research, 47(1), 1-15.

512 Smith, L., & DeWaard, C., 2005. Corrosion prediction and materials selection for oil
513 and gas producing environments. In CORROSION 2005. NACE International.

514 Straub D., Faber M.H., 2007, 'Temporal Variability in Corrosion Modeling and
515 Reliability Updating'. Journal of Offshore Mechanics and Arctic Engineering. Vol. 129 /
516 265.

517 Tarantseva, K. R., 2010. Models and methods of forecasting pitting corrosion.
518 Protection of metals and physical chemistry of surfaces, 46(1), 139-147.

519

520 Turnbull, A., 1993. 'Review of modelling of pit propagation kinetics'. British
521 Corrosion Journal, 28(4), 297-308. Volume 3, 2001, Pages 229-255.

522 Valor, A., Caleyó, F., Alfonso, L., Rivas, D., & Hallen, J. M. (2007a). Stochastic
523 modeling of pitting corrosion: a new model for initiation and growth of multiple corrosion
524 pits. Corrosion science, 49(2), 559-579.

525 Wang G., Spencer J., Elsayed T., 2003. Estimation of corrosion rates of structural
526 members in oil tankers. Proceedings of OMAE 2003 22nd International Conference on
527 Offshore Mechanics and Arctic Engineering. 8-13 June 2003, Cancun, Mexico.

528 Weijermars, R., 2013. Economic appraisal of shale gas plays in Continental Europe.
529 Applied Energy, 106, 100-115.

Williams D. E., Westcott C., Fleischmann M., 1985. Stochastic models of pitting corrosion of stainless steels I. Modeling of the initiation and growth of pits at constant potential. Journal of the Electrochemical Society, 132.8: 1796-1804.

Zhang S., Zhou W., 2014, Bayesian dynamic linear model for growth of corrosion defects on energy pipelines. Reliability Engineering and System Safety. 128(2014)24–31.

Zhang, G., Luo, J., Zhao, X., Zhang, H., Zhang, L., & Zhang, Y., 2012. Research on probabilistic assessment method based on the corroded pipeline assessment criteria. International Journal of Pressure Vessels and Piping, 95, 1-6.

Tables & Figures

Table 1 Overview of probabilistic distribution used in corrosion modelling

Author	pith depth	number of pits generated/area	time variation	spatial variation
Williams et al. (1985)	×	non-homogenous Poisson	✓	×
Laycock et al. (1990)	GEV	Exponential	Mean and standard deviation of GEV	×
Scarf&Laycock (1996)	GEV	GEV	Power law for mean and parameters	×
Turnbull (1993)	Exponential GEV	×	Power law for parameter GEV parameters	×
Melchers (2003d)	GEV	Weibull	Decreasing rate of pit generation over time	Poisson
Melchers (2005a,b)	Normal & Weighted Normal	×	Parameters vary over time	×
Engelhardt& Macdonald (2004),	Gumbel type I	Poisson	Non homogenous Poisson	Poisson
Isogai et al. (2004)	GEV	Poisson	×	×
Valor et al. (2007)	GEV	Gumbel	×	×
Caleyo et al (2009)	GEV	×	×	×
Jarrah et al. (2011)	Generalized Lambda	Poisson	Mean value of GLD	Poisson
Zhang et al (2012)	Normal	×	×	×
Zhang&Zhou (2014)	Weibull	Gamma	Bayesian Updating	×

Table 2 Normal distribution parameters for initiation time in years

Case	μ	σ
Field 1 OP-4.5in	2.80	0.50
Field 1 OP-5.5in	3.58	0.76
Field 2 OP-4.5in	3.03	1.26
Field 2 OP-5.5in	1.96	0.26

Table 3 Constants calibrated on the data for the linear function $\lambda(t)$

Case	a	b
Field 1 OP-4.5in	-0.0093	0.004
Field 1 OP-5.5in	-0.0098	0.0041
Field 2 OP-4.5in	-0.00038	0.0018
Field 2 OP-5.5in	-0.0013	0.002

Table 4 Gaussian mixture model parameters

Case	Ncomp	weight	μ [in]	σ [in]
Field 1 OP-4.5in	Φ_1	0.2727	0.0727	$0.4126 \cdot 10^{-4}$
	Φ_2	0.7273	0.0196	$0.4126 \cdot 10^{-4}$
Field 1 OP-5.5in	Φ_1	0.8030	0.0422	$2.811 \cdot 10^{-4}$
	Φ_2	0.1970	0.1130	$2.811 \cdot 10^{-4}$
Field 2 OP-4.5in	Φ_1	0.7877	0.0239	$0.630 \cdot 10^{-4}$
	Φ_2	0.2123	0.0722	$0.630 \cdot 10^{-4}$
Field 2 OP-5.5in	Φ_1	0.8618	0.0390	$3.136 \cdot 10^{-4}$
	Φ_2	0.1382	0.1273	$3.136 \cdot 10^{-4}$

Table 5 BHP and THP parameters (in psi) of the marginal distributions for Field 1 with correlation coefficient ρ

Variable	Symbol	Distribution	p1	p2	ρ
Pressure Yearly maxima w_p	BHP	WB	2506.7	3.012	0.388
	THP	WB	1731.8	1.465	

Table 6 BHP and THP parameters (in psi) of the marginal distributions for Field 2 with correlation coefficient ρ

Variable	Symbol	Distribution	p1	p2	ρ
Pressure Yearly maxima w_p	BHP	WB	2879	4.409	0.415
	THP	WB	1437	2.483	

Table 7 Stochastic variables of failure model

Variable	Symbol	Distribution	μ	c.o.v.
Initiation Time	I_t	See Table 2	-	-
Pit depth [in]	d_p	See Table 4	-	-
Diameter [in]	D	Deterministic	4.5	-
			5.5	-
Nominal wall thickness [in]	t_n	Deterministic	0.271 0.361	-

Pit length [in]	l	Normal	$2d_p$	0.05
Factor m_f	m_f	LogN	1.1	0.05
Material Yield stress [psi]	σ_y	LogN	80000	0.05
Fluid Pressure [psi]	p_s	See Table 5 & Table 6	-	-
Gaussian increment	ω_T	Normal	0	0.56 0.48
Gaussian increment	ω_B	Normal	0	0.58 0.25

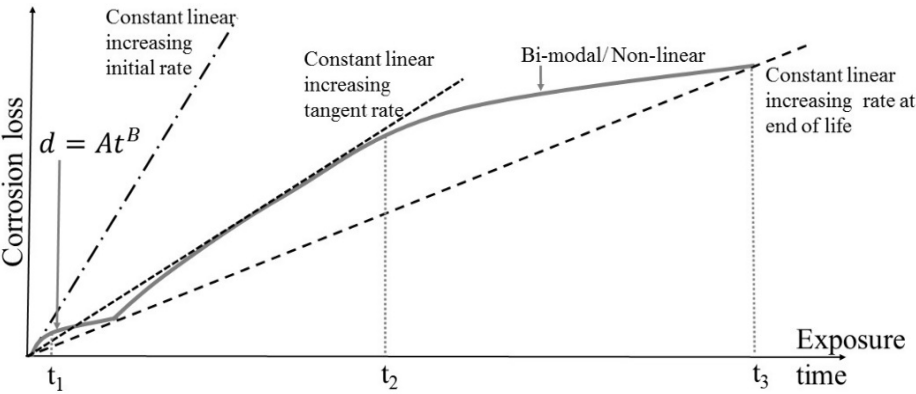


Figure 1. Phenomenological evolution of corrosion losses (Melchers, 2003a)

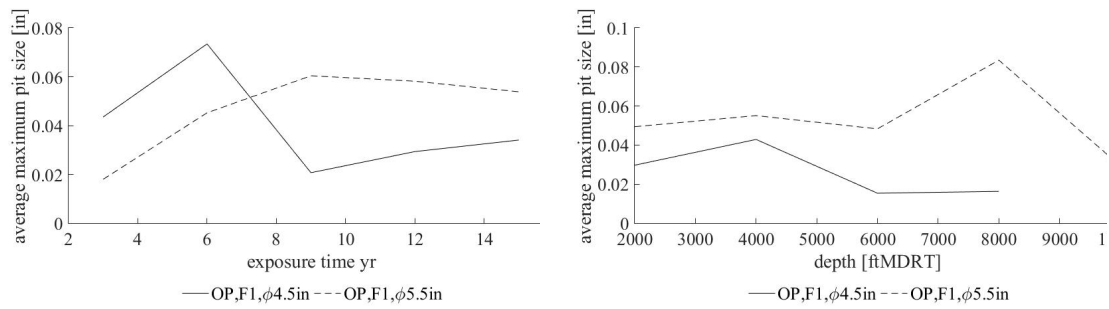


Figure 2 Average of maximum pit size measured over exposure time (left) and depth (right) for Field 1

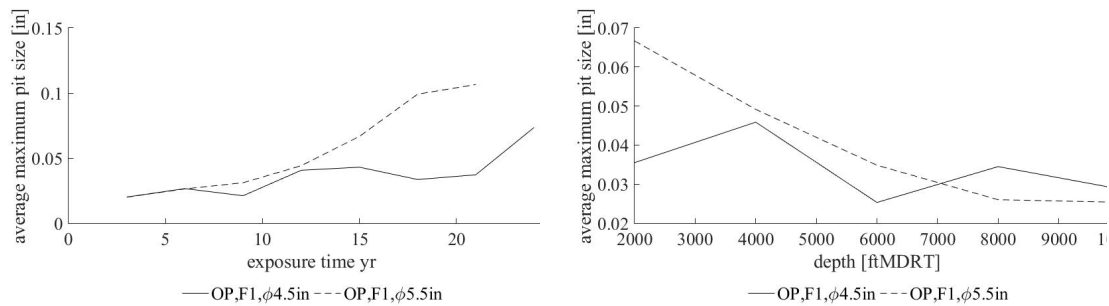


Figure 3 Average of maximum pit size measured over exposure time (left) and depth (right) for Field 2

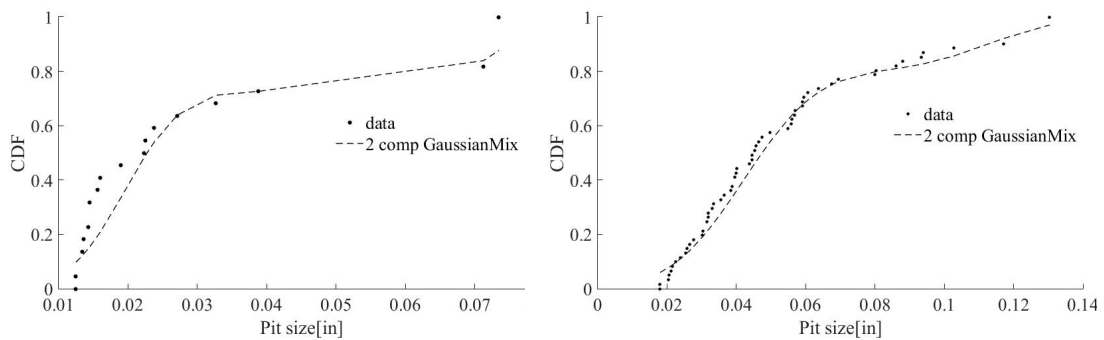


Figure 4 CDF of maximum pit size for OP-Field1-4.5in (left) and OP-Field1-5.5in (right)

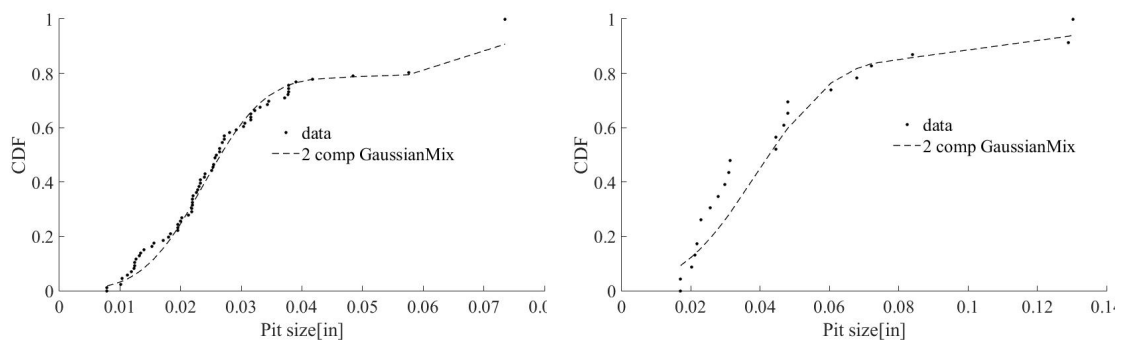
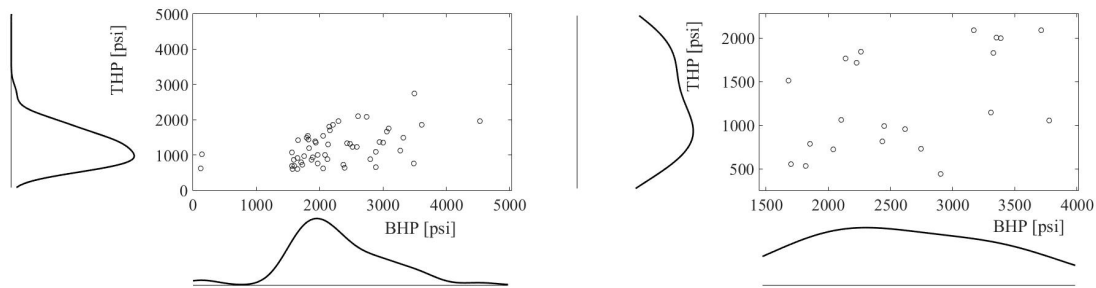
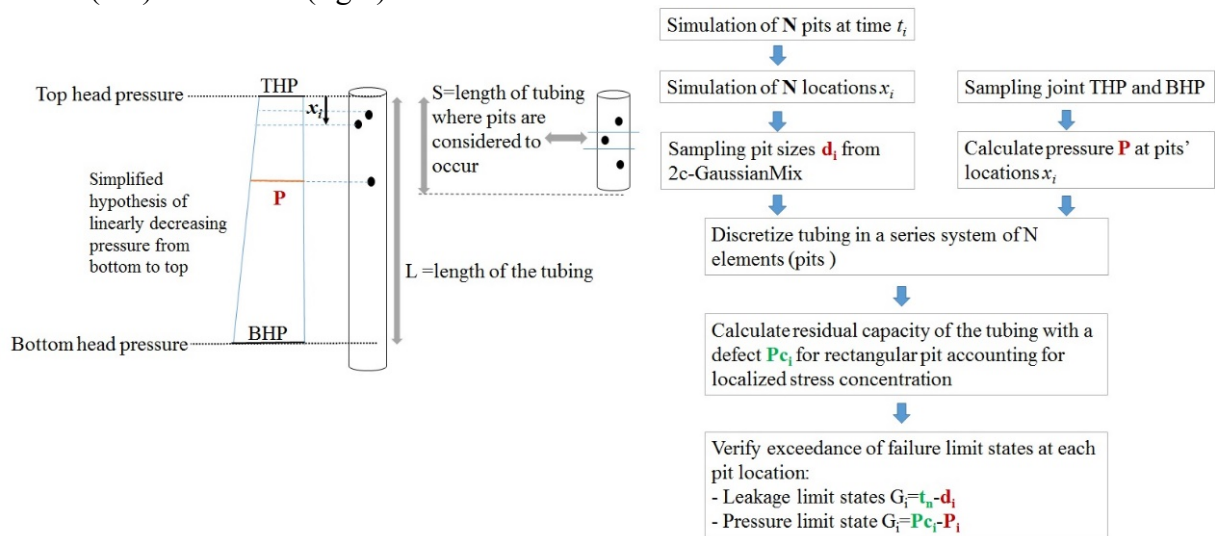


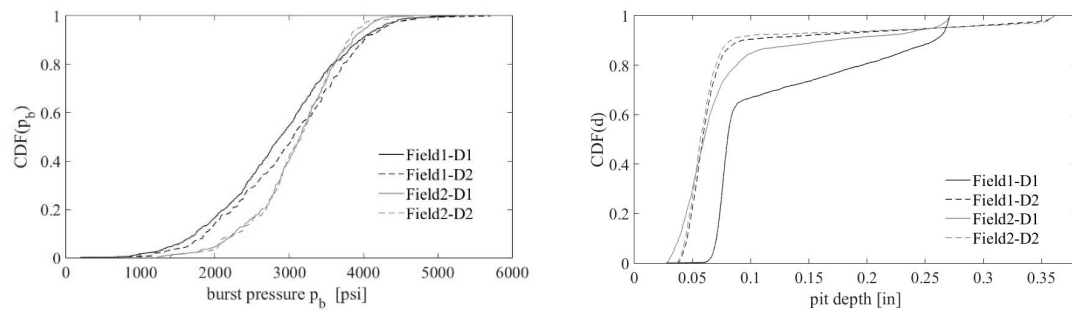
Figure 5 CDF of maximum pit size for OP-Field2-4.5in (left) and OP-Field2-5.5in (right)



575 Figure 6 Empirical marginal density functions for yearly maxima of BHP and THP for
576 Field 1(left) and Field 2(right)



577 Figure 7 Illustration of simulation model
578
579
580



581 Figure 8 Cumulative probability of (left) burst pressure at failure and (right) pit size at
582 failure
583

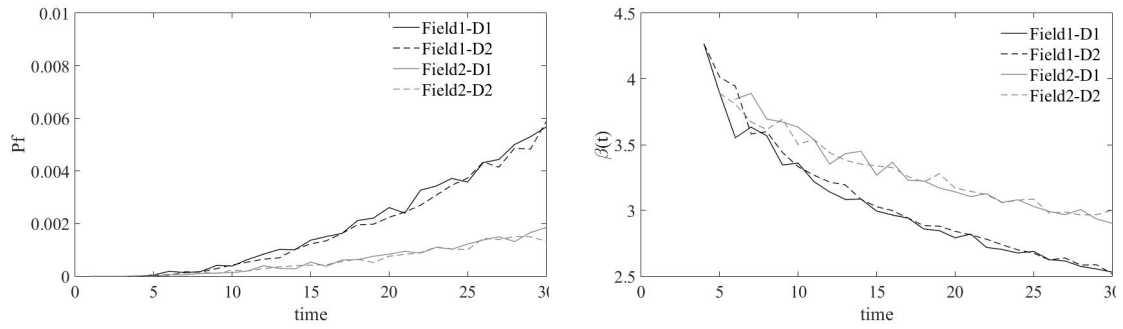


Figure 9 Cumulative probability of burst failure (left) and reliability index (right) for corrective maintenance

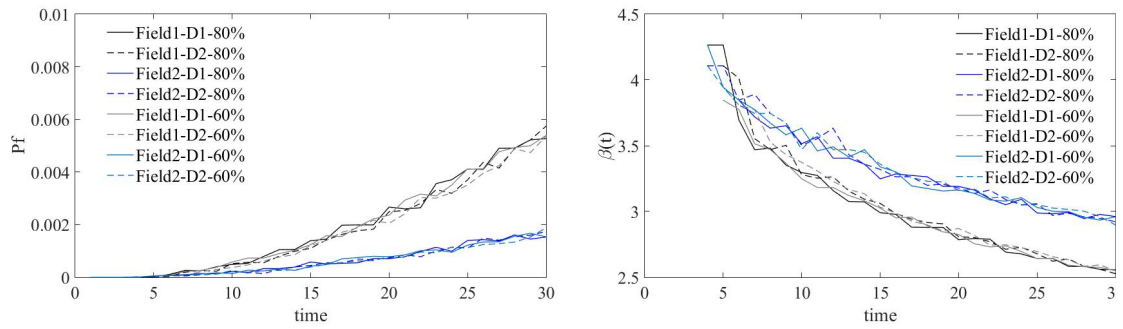


Figure 10 Cumulative probability of failure (left) and reliability index (right) for condition based maintenance (3yr) with thresholds of 60% and 80%

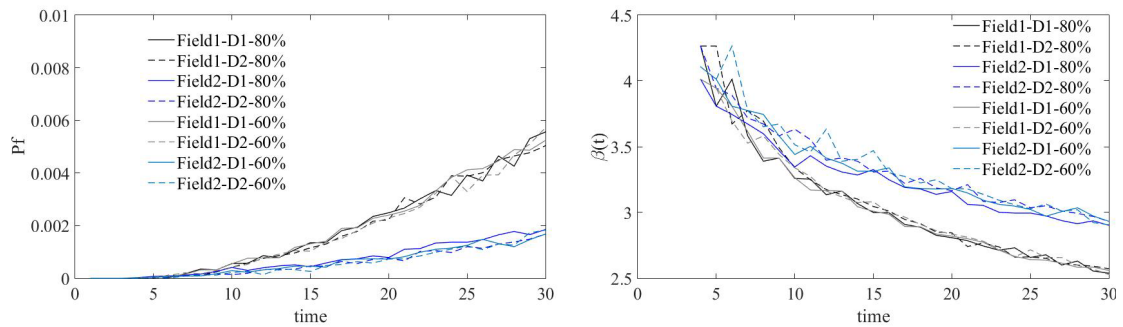


Figure 11 Cumulative probability of failure (left) and reliability index (right) for condition based maintenance (10yr) with threshold of 60% and 80%

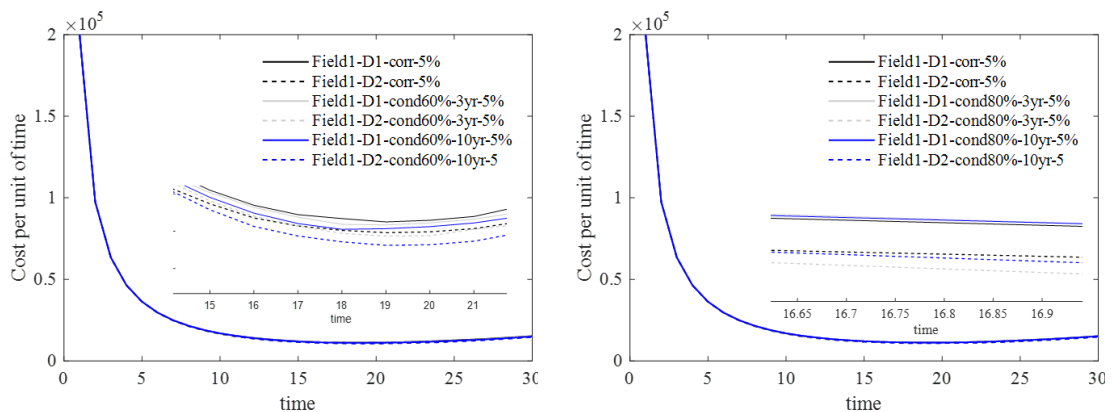


Figure 12 Cost per unit of time for corrective (corr) and condition based maintenance (cond) at 3yr and 10yr inspection interval with threshold of defect size at 60% (left) and 80% (right) thickness, 5% discount rate and $F_c = 3 \times WO$

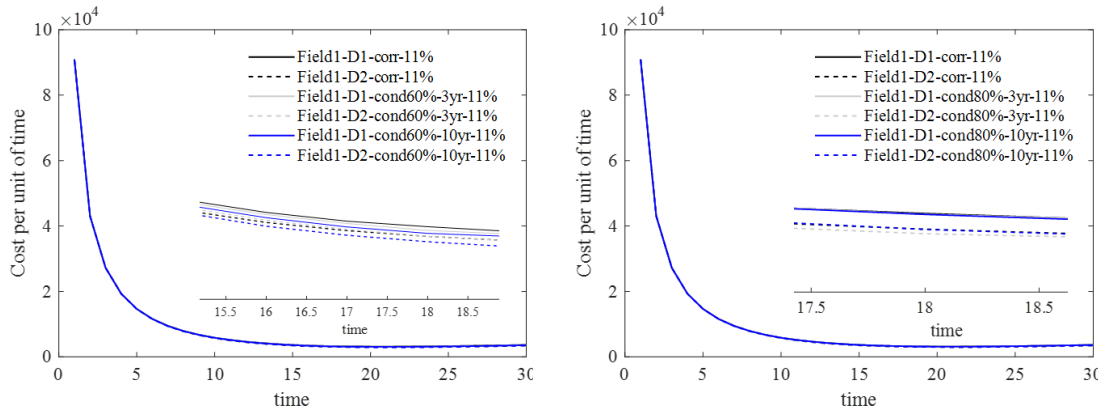


Figure 13 Cost per unit of time for corrective (corr) and condition based maintenance (cond) at 3yr and 10yr inspection interval with threshold of defect size at 60% (left) and 80% (right) thickness, 11% discount rate and $F_c = 3 \times WO$

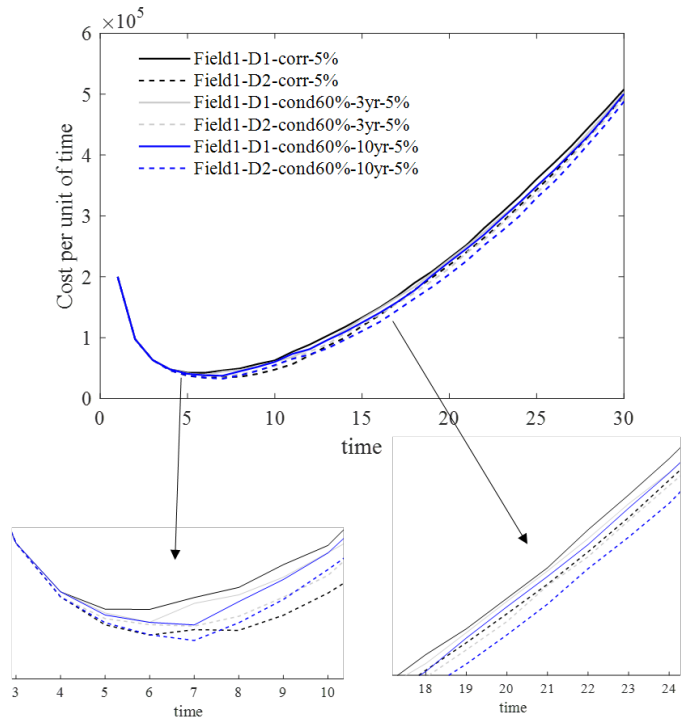
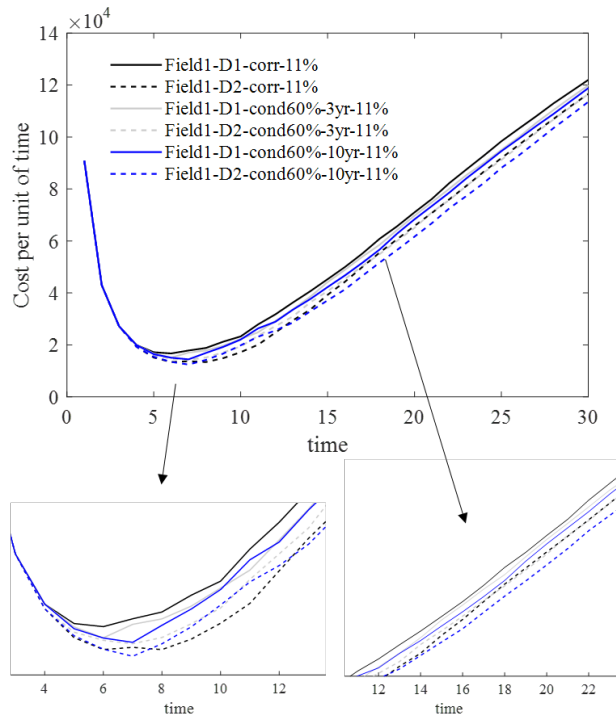


Figure 14 Cost per unit of time for corrective (corr) and condition based maintenance (cond) at 3yr and 10yr inspection interval with threshold of defect size at 60% thickness, 5% discount rate and $F_c = 100 \times WO$



601

602 Figure 15 Cost per unit of time for corrective (corr) and condition based maintenance
 603 (cond) at 3yr and 10yr inspection interval with threshold of defect size at 60% thickness,
 604 11% discount rate and $F_c = 100 \cdot W_O$
 605